JACS
JOURNAL OF THE AMERICAN CHEMICAL SOCIETY
pubs.acs.org/JACS
Communication

A Manganese Compound I Model with a High Reactivity in the Oxidation of Organic Substrates and Water

Lina Zhang, Mi Sook Seo, Yunhee Choi, Roman Ezhov, Olga Maximova, Deesha D. Malik, Maggie Ng, Yong-Min Lee, Ritimukta Sarangi,* Yulia N. Pushkar,* Kyung-Bin Cho,* and Wonwoo Nam*

Cite This: https://doi.org/10.1021/jacs.3c01818
Read Online
ACCESS | Metrics & More | Article Recommendations | Supporting Information

ABSTRACT: A high-valent manganese(IV)-hydroxo porphyrin π-cation radical complex, $[Mn(IV)(OH)(Porp^{+\bullet})(X)]^{+}$, was synthesized and characterized spectroscopically. The Mn porphyrin intermediate was highly reactive in alkane hydroxylation and oxygen atom transfer reactions. More importantly, the Mn porphyrin intermediate reacted with water at a fast rate, resulting in the dioxygen evolution. To the best of our knowledge, we report the first manganese Cpd I model compound bearing a porphyrin π-cation radical ligand with a high reactivity in oxidation reactions, including water oxidation.

Heme enzymes, such as cytochromes P450, peroxidases, and catalases, utilize high-valent iron(IV)-oxo porphyrin π-cation radicals, referred to as compound I (Cpd I), as reactive intermediates in various oxidation reactions.[1] As biomimetic models of Cpd I, a number of iron(IV)-oxo porphyrin π-cation radicals, $[Fe^{IV}(O)(Porp^{+\bullet})]^{+}$, have been synthesized, characterized, and investigated in oxidation reactions, including C−H bond activation and oxygen atom transfer (OAT) reactions.[2] High-valent manganese-oxo porphyrin complexes have also been investigated extensively as an analogue of Cpd I models.[2,3] However, different from the Cpd I models, only manganese(V)-oxo porphyrin complexes, $[Mn^{V}(O)(Porp)]^{+}$, but not manganese(IV)-oxo porphyrin π-cation radicals, $[Mn^{IV}(O)(Porp^{+\bullet})]^{+}$, have been reported.[3−6]

In photosystem II, a manganese(V)-oxo intermediate has been proposed to participate in the energy-demanding O−O bond formation, which is the most crucial step in the dioxygen evolution at the oxygen-evolving complex.[7] Therefore, tremendous efforts have been devoted to capturing highly reactive Mn(V)-oxo species and elucidating mechanism(s) of the O−O bond formation by the intermediate(s) in catalytic water oxidation reactions. While the O−O bond formation between manganese(V)-oxo corroles and hydroxide (OH^{-}) was reported,[8] the O_2 evolution in the reaction of a high-valent manganese-oxo complex and water has never been observed previously.

Herein, we report for the first time the synthesis, characterization, and reactivity studies of a Mn(IV)-hydroxo porphyrin π-cation radical complex (**2**, Scheme 1). **2** is highly reactive in the C−H bond activation of alkanes, including the hydroxylation of cyclohexane to cyclohexanol, and OAT reactions (Scheme 1C). Surprisingly, **2** reacts with H_2O to afford O_2 evolution (Scheme 1C).

A Mn(IV)-oxo porphyrin complex, $[Mn^{IV}(O)(TDCPP)]$ (**1**),[9] was synthesized by reacting $[Mn^{III}(TDCPP)(Cl)]$ with $^{S}PhIO$[9] (5 equiv) in CH_2Cl_2 at −10 °C (Scheme 1A).[10] Addition of HOTf (10 equiv) to a solution of **1** generated a

Scheme 1. Synthesis and Characterization of Mn(IV)-Hydroxo Porphyrin π-Cation Radical Complex (2) and Its Oxidation Reactions

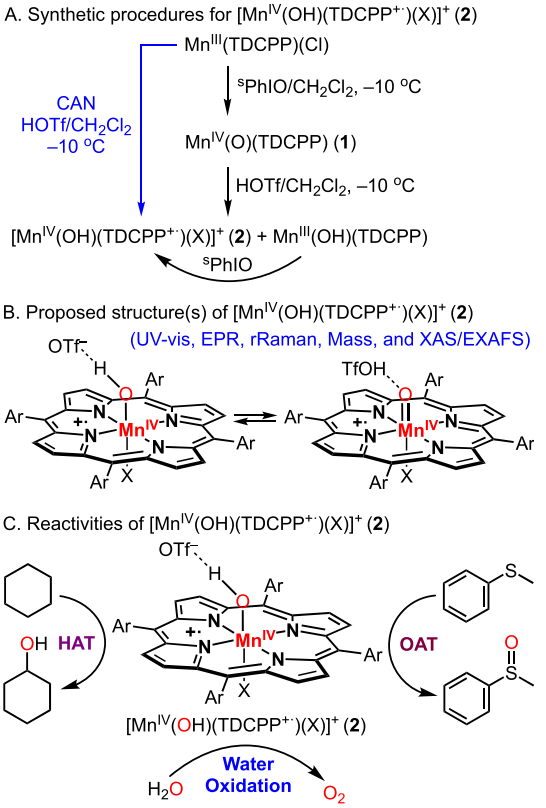

Received: February 18, 2023

https://doi.org/10.1021/jacs.3c01818
J. Am. Chem. Soc. XXXX, XXX, XXX−XXX

green-colored intermediate, denoted as **2**, exhibiting a Soret band at 390 nm with a reduced intensity and the broad Q-band at 674 nm (Figure 1; SI, Experimental Section); such spectral

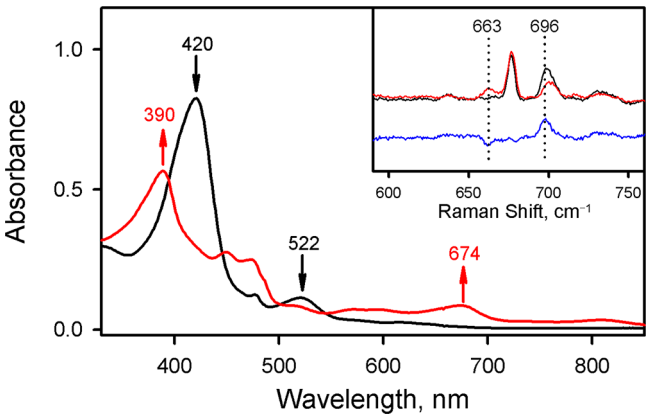

Figure 1. UV−vis spectral change showing the formation of **2** (red) by adding HOTf (1.0 mM) to **1** (0.10 mM, black) in CH_2Cl_2 at −10 °C. Inset shows rRaman spectra of **2** (black) and **2**-^{18}O (red) and their difference spectrum (blue).

features of the Soret and Q-bands suggest that a Mn species bearing a porphyrin π-cation radical ligand was generated via a disproportionation process (Scheme 1A),[11] as demonstrated in iron porphyrin and TAML systems.[12−14] **2** was also generated by reacting [Mn^{III}(TDCPP)(Cl)] with CAN[9] (4 equiv) in the presence of HOTf in CH_2Cl_2 at −10 °C (Scheme 1A, blue-colored reaction) (Figure S1). **2** reverted to **1** upon addition of base (e.g., tetramethylammonium hydroxide), and further addition of protons to the resulting solution of **1** regenerated **2** and Mn(III) complexes (Figure S2).[15] **2** was metastable at −10 °C and decomposed to a Mn(III) species (Figures S3−S5). Its stability depends on the amount of HOTf ($t_{1/2}$ = ∼60 s with 2 equiv and ∼1500 s with 10 equiv) (Figures S3 and S6). Therefore, **2** was generated using 10 equiv of HOTf in the spectroscopic characterization and reactivity studies.

CSI-MS[9] of **2** exhibited a peak at a mass-to-charge ratio (m/z) of 1057.9 with mass and isotope distribution patterns corresponding to [Mn(O)(TDCPP)(CF_3CH_2O)] (Figure S7b). Since **2** reacted with water, we were not able to achieve the ^{18}O-labeled Mn-oxo species using $H_2{}^{18}O$ (Figure S7c).[16] However, the rRaman[9] spectrum of **2** (λ_{ex} = 442 nm) in frozen CH_3CN−CH_2Cl_2 exhibited a band at 696 cm^{-1}, which shifted to 663 cm^{-1} upon ^{18}O-substitution (Figure 1, inset; Experimental Section; Figure S8b). The observed isotopic shift of −33 cm^{-1} with ^{18}O-substitution is in good agreement with the calculated value (−31 cm^{-1}) for a diatomic Mn−O oscillator. Although the Mn−O stretching frequency is lower than the typical metal-oxo double-bond frequencies (e.g., ∼800 cm^{-1}),[17] there are several examples of metal-oxo complexes with M−O stretches at 670−700 cm^{-1} when the metal-oxo complexes bind Lewis acidic metal ions (e.g., Ce^{IV}).[18] It is also noted that several Mn(IV)-hydroxo complexes with Mn−O vibrational data of 660−680 cm^{-1} and Mn−O bond lengths of ∼1.80 Å have been reported in nonheme and porphyrinoid Mn systems.[19] The EPR[9] spectrum of **2** was silent (Figure S9). Since the starting Mn(III) porphyrin complex was also EPR silent, we performed a redox-titration experiment with one-electron reductants, such as [Ru(5-Cl-phen)$_3$]$^{2+}$ (E_{ox} vs SCE = 1.41 V) and [Ru(5-NO_2-phen)$_3$]$^{2+}$ (E_{ox} vs SCE = 1.50 V), and found that 2 equiv of one-electron reductants was required for the full conversion of **2** to [Mn^{III}(TDCPP)]$^+$ (Figure S10). The latter result indicates that **2** is a two-electron-oxidized species of the Mn(III) porphyrin complex. XAS/EXAFS[9] of **2** is shown in Figure 2. In the Mn K-edge XANES[9] spectra of

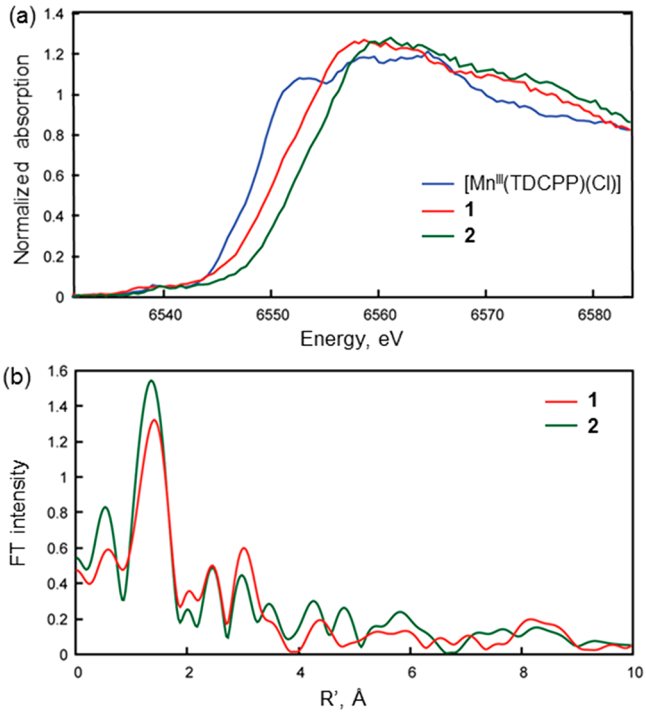

Figure 2. (a) Mn K-edge XANES of [Mn^{III}(TDCPP)(Cl)], **1**, and **2** in CH_3CN/TFE (v/v 20:1). (b) Non-phase-shift-corrected Fourier transformation (FT) data of **1** and **2**.

[Mn^{III}(TDCPP)(Cl)] and **1**, the high energy shift is in agreement with Mn^{III} to Mn^{IV} oxidation. XAS data of **1** are in agreement with the earlier results (Table S1).[20a] Treatment of **1** with HOTf (10 equiv) results in further shift of XANES by ∼2 eV, in agreement with the proposed formation of a Mn(IV) species with a porphyrin π-cation radical ligand for **2** (vide infra). **2** has an edge position similar to the previously reported [Mn^{V}(TDCPP)(O)]$^+$ and a five-coordinate [Mn^{V}(HMPAB)-(O)]$^-$.[9,20a,b] It is also similar to five-coordinate [Mn^{V}(TPFC)-(O)]$^+$ generated by reacting [Mn^{III}(TPFC)][9] and PhIO (Figure S11).[20c] Low pre-edge intensity of **2** (Figure 2a) requires an increase in coordination number in comparison to the five-coordinate Na[Mn^{V}(HMPAB)(O)] complex.[20b] The presence of a strong *trans*-axial ligand would weaken the Mn^{V}-oxo bond (thus lowering 4pz mixing) and would also shift the Mn more into the equatorial plane, resulting in a more centrosymmetric Mn center. All such factors contribute to a reduced electric dipole contribution and a weaker pre-edge intensity in **2** (Figure 2a). EXAFT fits (Tables S1 and S2; Figure S12) for **1** and **2** indicate similar Mn−O distances at ∼1.75 Å with some shortening of the Mn−N distances from ∼1.98 Å to 1.94 Å in **2**. We did not observe the Mn−Cl interaction in the EXAFS, and addition of a Mn−Cl shell in the 2.1−2.3 Å interval did not improve the EXAFS fits.

2 was further investigated by DFT (Tables S3−S17). Figure 3 summarizes the DFT-based model best fit to the experimental data. It features an OTf$^-$ axial ligand, as XAS indicated a six-coordinate complex but no chloride ion ligand.

https://doi.org/10.1021/jacs.3c01818
J. Am. Chem. Soc. XXXX, XXX, XXX−XXX

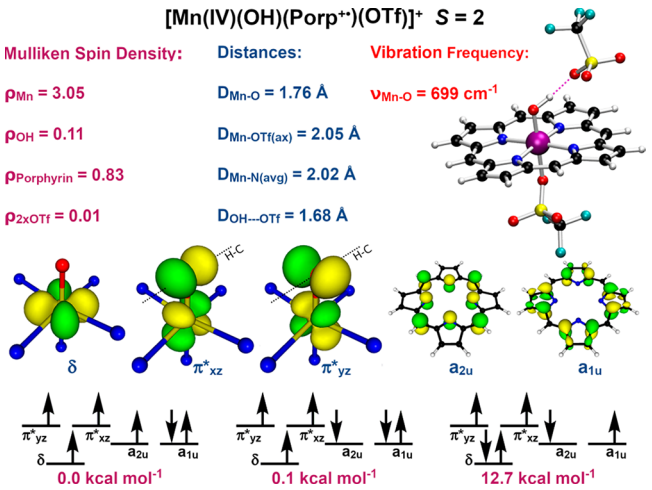

Figure 3. DFT-calculated $[Mn^{IV}(OH)(Porp^{+\bullet})(OTf)]^{+}$ species with an OTf^{-} molecule hydrogen bonded to the Mn-hydroxo moiety. Selected Mulliken spin density distributions, distances, and the Mn−O vibration frequency for the $S = 2$ species are shown. The electronic configurations for the lowest quintet and triplet are shown, along with a high-energy 4-radicaloid triplet found.

The EXAFS bond length of 1.75 Å is between the calculated double-bond Mn−O distance (1.65 Å, Figure S13) and the single-bond Mn−OH distance (1.79 Å, Table S8). Placing an OTf^{-} at a hydrogen-bonding distance (i.e., increasing the oxo character by forming Mn−OH---OTf^{-}) caused the distance to drop to 1.76 Å (Table S5). The calculated Mn−O vibration frequency on this hydrogen-bonded species is 699 cm^{-1}, significantly closer to the experimental value (696 cm^{-1}) than the bare Mn−O (889 cm^{-1}) or Mn−OH (641 cm^{-1}). A porphyrin radical is indeed seen to be present (Table S4). Since this porphyrin radical is only weakly coupled to the spins on the Mn−O moiety, it can be both antiferromagnetically and ferromagnetically coupled with only a negligible change in the overall energy. Thus, it is seen that the compound spin state is virtually energetically degenerate between the overall triplet and quintet (Table S3). Based on the spectroscopic data, such as the Mn−O stretch from rRaman and the Mn−O bond distance from EXAFS, and the computational calculations,[17] we propose **2** as a manganese(IV)-hydroxo porphyrin π-cation radical complex, $[Mn^{IV}(OH)(Porp^{+\bullet})(X)]^{+}$; a possibility of **2** being a manganese(IV)-oxo porphyrin π-cation radical complex interacting noncovalently with a proton at the Mn-oxo moiety, $[Mn^{IV}(O)(Porp^{+\bullet})(X)-(HOTf)]$, cannot be excluded (see the structures in Scheme 1B).[21,22]

We then investigated the reactivity of **2** in the C−H bond activation of alkanes. In the reaction of **2** with cyclohexane, the absorption peak at 674 nm due to **2** disappeared with the formation of the peak at 478 nm due to Mn(III) porphyrin (Figure 4a). The reaction rate increased linearly with increasing the substrate concentration, affording second-order rate constants (k_2) of 3.4×10^{-3} M^{-1} s^{-1} for cyclohexane and 1.5×10^{-3} M^{-1} s^{-1} for deuterated cyclohexane (cyclohexane-d_{12}) to give a KIE[9] value of 2.3 (Figure 4a, inset).[23] The reactivity of **2** was also studied with other alkanes, such as cycloheptane, cyclooctane, and cyclopentane (Table S18; Figure S14), and a good linear correlation between $\log(k_2')$ values and the C−H BDEs[9,24] of the substrates was observed (Figure 4b). Product analysis of the cyclohexane oxidation by **2** revealed the formation of cyclohexanol (37%). Similarly, the

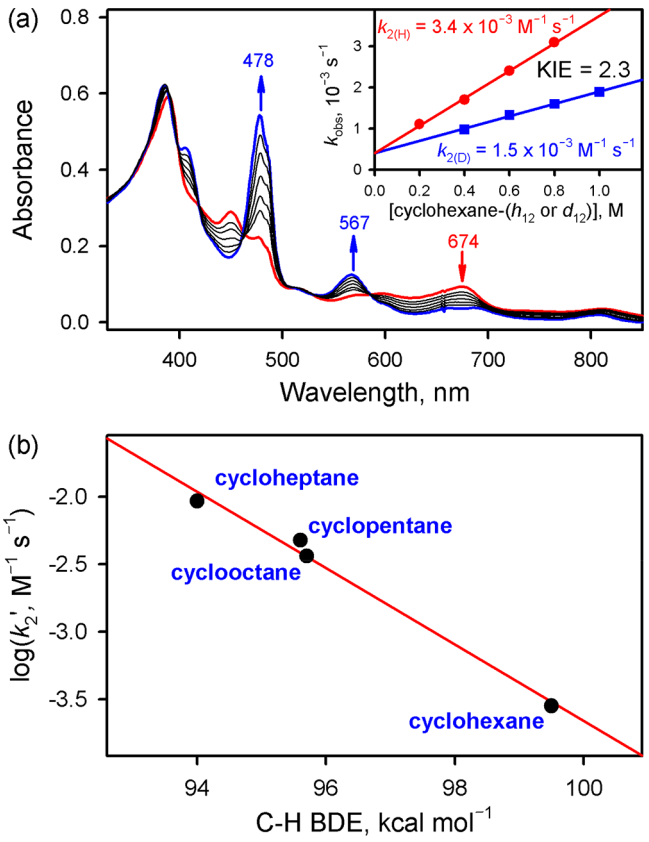

Figure 4. (a) UV−vis spectral changes observed in the reaction of **2** (0.10 mM, red) and cyclohexane (0.20 M) in CH_2Cl_2/CH_3CN (v/v 20:1) at −10 °C. Inset shows the plots of k_{obs} against concentrations of cyclohexane-h_{12} (red) and cyclohexane-d_{12} (blue). (b) Plot of log k_2' ($k_2' = k_2$/number of equivalent target C−H bonds) against the C−H BDEs of substrates.

products formed in the oxidation of cycloheptane by **2** were cycloheptanol (65%) and cycloheptanone (12%) (Table S19) and Mn(III) porphyrin as an inorganic product (Figure S15). When cycloheptane oxidation was performed with ^{18}O-labeled **2**, the ^{18}O percent in the cycloheptanol product was ∼50% (Figure S16). Thus, the results presented above are similar to those observed in alkane hydroxylation reactions by Cpd I models,[1,2,25] but are different from the oxidation of hydrocarbons by **1**, in which chlorinated products were yielded in halogenated solvents.[10]

In OAT reactions, we investigated the oxidation of *para*-X-substituted thioanisoles by **2**. Since the reaction of **2** with thioanisole was too fast to follow even with a stopped-flow UV−vis spectrophotometer (Figure S17), *para*-X-substituted thioanisoles with an electron-withdrawing substituent were used as substrates to determine second-order rate constants (k_2), such as 82 M^{-1} s^{-1} for 4-NO_2-thioanisole, 1.9×10^2 M^{-1} s^{-1} for 4-CHO-thioanisole, and 6.3×10^2 M^{-1} s^{-1} for 4-CN-thioanisole at −40 °C (Figure S18), with the result that **2** was found to be an electrophile with a large negative slope (ρ = −6.8) in the Hammett plot (Figure S19). Further, **2** was much more reactive (∼10^5 times) than **1** in the oxidation of 4-CN-thioanisole (5.7×10^{-3} M^{-1} s^{-1} for **1** at −40 °C) (Figures S18c and S20). Product analysis for the thioanisole oxidation by **2** revealed the formation of sulfoxide (∼98% yield based on **2**) and Mn(III) porphyrin (Figure S17). When an ^{18}O-labeled water experiment was performed with **2**-^{18}O in situ generated

https://doi.org/10.1021/jacs.3c01818
J. Am. Chem. Soc. XXXX, XXX, XXX−XXX

in the presence of $H_2{}^{18}O$, the amount of ^{18}O-incorporation in the sulfoxide product was found to be dependent on the amount of $H_2{}^{18}O$ present in the reaction solution (Experimental Section, Figure S21).

As briefly discussed above, **2** was unstable in the presence of water. When a small amount of H_2O was added to **2**, **2** was converted to a Mn(III) porphyrin complex (Figure 5a). The

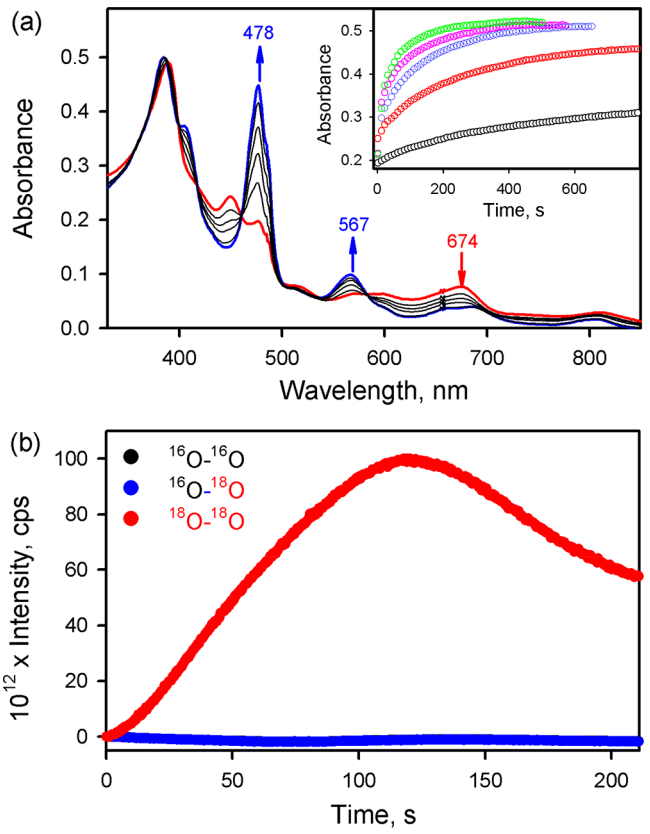

Figure 5. (a) UV−vis spectral changes observed upon addition of H_2O to **2** (0.10 mM, red) in CH_2Cl_2/CH_3CN (v/v 20:1) at −10 °C. Inset shows time traces monitored at 478 nm with different H_2O concentration [0 (black), 20 (red), 40 (blue), 60 (pink), and 80 mM (green)]. (b) Time profiles of mass spectra of O_2 isotopes produced in the reaction of ^{18}O-labeled **2** and $H_2{}^{18}O$ in deaerated CH_3CN/CH_2Cl_2 (v/v 8:1) at −40 °C.

disappearance of **2** became faster with increasing H_2O concentration (Figure 5a, inset), and a second-order rate constant (k_2) was determined to be 1.9×10^{-1} M^{-1} s^{-1} at −10 °C (Figure S22a). We also found that a significant amount of O_2 (33% yield based on **2**) was evolved in the reaction (Experimental Section, Figures S23−S25). When ^{18}O-enriched water ($H_2{}^{18}O$) was used, $^{18}O_2$ was evolved (Figure 5b). In contrast to **2**, **1** and the Cpd I model analogue, $[Fe^{IV}(O)(TDCPP^{+\bullet})]^+$, did not react with water (Figure S26). Detailed mechanistic studies are underway in this laboratory to elucidate the mechanism of the O−O bond formation between **2** and water.[26]

In conclusion, we have reported a heme Cpd I-like Mn intermediate bearing a porphyrin π-cation radical ligand. Reactivity studies revealed that this Mn Cpd I intermediate is highly reactive in C−H bond activation and OAT reactions. Surprisingly, the Mn Cpd I intermediate reacts with water to evolve O_2. Our future studies will focus on fully understanding the physicochemical properties of Mn Cpd I models and the mechanism of the O−O bond formation between Mn Cpd I models and H_2O.

■ ASSOCIATED CONTENT

Supporting Information

The Supporting Information is available free of charge at https://pubs.acs.org/doi/10.1021/jacs.3c01818.

Experimental Section, Tables S1−S19, and Figures S1−S26 (PDF)

■ AUTHOR INFORMATION

Corresponding Authors

Wonwoo Nam − *Department of Chemistry and Nano Science, Ewha Womans University, Seoul 03760, Korea; State Key Laboratory for Oxo Synthesis and Selective Oxidation, Lanzhou Institute of Chemical Physics, Chinese Academy of Sciences, Lanzhou 730000, China;* orcid.org/0000-0001-8592-4867; Email: wwnam@ewha.ac.kr

Kyung-Bin Cho − *Department of Chemistry, Jeonbuk National University, Jeonju 54896, Korea;* orcid.org/0000-0001-6586-983X; Email: workforkyung@jbnu.ac.kr

Yulia N. Pushkar − *Department of Physics, Purdue University, West Lafayette, Indiana 47907, United States;* orcid.org/0000-0001-7949-6472; Email: ypushkar@purdue.edu

Ritimukta Sarangi − *Stanford Synchrotron Radiation Lightsource, SLAC National Accelerator Laboratory, Stanford, California 94025, United States;* orcid.org/0000-0002-2764-2279; Email: ritis@slac.stanford.edu

Authors

Lina Zhang − *Department of Chemistry and Nano Science, Ewha Womans University, Seoul 03760, Korea;* orcid.org/0000-0003-4539-2741

Mi Sook Seo − *Department of Chemistry and Nano Science, Ewha Womans University, Seoul 03760, Korea;* orcid.org/0000-0003-3302-2508

Yunhee Choi − *Department of Chemistry, Jeonbuk National University, Jeonju 54896, Korea*

Roman Ezhov − *Department of Physics, Purdue University, West Lafayette, Indiana 47907, United States;* orcid.org/0000-0001-6806-4033

Olga Maximova − *Department of Physics, Purdue University, West Lafayette, Indiana 47907, United States;* orcid.org/0000-0001-7789-6683

Deesha D. Malik − *Department of Chemistry and Nano Science, Ewha Womans University, Seoul 03760, Korea;* orcid.org/0000-0001-7800-8852

Maggie Ng − *Department of Chemistry, Jeonbuk National University, Jeonju 54896, Korea;* orcid.org/0000-0002-0656-3002

Yong-Min Lee − *Department of Chemistry and Nano Science, Ewha Womans University, Seoul 03760, Korea;* orcid.org/0000-0002-5553-1453

Complete contact information is available at: https://pubs.acs.org/10.1021/jacs.3c01818

Notes

The authors declare no competing financial interest.

https://doi.org/10.1021/jacs.3c01818
J. Am. Chem. Soc. XXXX, XXX, XXX−XXX

■ ACKNOWLEDGMENTS

This work was supported by the NRF of Korea (NRF-2021R1A3B1076539 to W.N., NRF-2020R1I1A1A01074630 to Y.-M.L., and NRF-2021R1A2C1012851 to K.-B.C). This research was also supported by NSF CHE-2004147 to Y.P. The use of the Advanced Photon Source, an Office of Science User Facility operated by the U.S. Department of Energy (DOE) Office of Science by Argonne National Laboratory, was supported by the U.S. DOE under Contract DE-AC02-06CH11357. The PNC/XSD (Sector 20) facilities at the Advanced Photon Source and research at these facilities were supported by the U.S. Department of Energy, Basic Energy Science, and the Canadian Light Source.

■ REFERENCES

(1) (a) Dubey, K. D.; Shaik, S. Cytochrome P450−The Wonderful Nanomachine Revealed through Dynamic Simulations of the Catalytic Cycle. *Acc. Chem. Res.* **2019**, *52*, 389−399. (b) Moody, P. C. E.; Raven, E. L. The Nature and Reactivity of Ferryl Heme in Compounds I and II. *Acc. Chem. Res.* **2018**, *51*, 427−435. (c) Guengerich, F. P. Mechanisms of Cytochrome P450-Catalyzed Oxidations. *ACS Catal.* **2018**, *8*, 10964−10976. (d) Krest, C. M.; Onderko, E. L.; Yosca, T. H.; Calixto, J. C.; Karp, R. F.; Livada, J.; Rittle, J.; Green, M. T. Reactive Intermediates in Cytochrome P450 Catalysis. *J. Biol. Chem.* **2013**, *288*, 17074−17081. (e) Ortiz de Montellano, P. R. Hydrocarbon Hydroxylation by Cytochrome P450 Enzymes. *Chem. Rev.* **2010**, *110*, 932−948.

(2) (a) Guo, M.; Corona, T.; Ray, K.; Nam, W. Heme and Nonheme High-Valent Iron and Manganese Oxo Cores in Biological and Abiological Oxidation Reactions. *ACS Cent. Sci.* **2019**, *5*, 13−28. (b) Sacramento, J. J. D.; Goldberg, D. P. Factors Affecting Hydrogen Atom Transfer Reactivity of Metal−Oxo Porphyrinoid Complexes. *Acc. Chem. Res.* **2018**, *51*, 2641−2652. (c) Huang, X.; Groves, J. T. Oxygen Activation and Radical Transformations in Heme Proteins and Metalloporphyrins. *Chem. Rev.* **2018**, *118*, 2491−2553. (d) Baglia, R. A.; Zaragoza, J. P. T.; Goldberg, D. P. Biomimetic Reactivity of Oxygen-Derived Manganese and Iron Porphyrinoid Complexes. *Chem. Rev.* **2017**, *117*, 13320−13352. (e) Fujii, H. Electronic Structure and Reactivity of High-Valent Oxo Iron Porphyrins. *Coord. Chem. Rev.* **2002**, *226*, 51−60.

(3) Liu, W.; Groves, J. T. Manganese Catalyzed C-H Halogenation. *Acc. Chem. Res.* **2015**, *48*, 1727−1735.

(4) (a) Jin, N.; Ibrahim, M.; Spiro, T. G.; Groves, J. T. Trans-dioxo Manganese(V) Porphyrins. *J. Am. Chem. Soc.* **2007**, *129*, 12416−12417. (b) De Angelis, F.; Jin, N.; Car, R.; Groves, J. T. Electronic Structure and Reactivity of Isomeric Oxo-Mn(V) Porphyrins: Effects of Spin-State Crossing and pK_a Modulation. *Inorg. Chem.* **2006**, *45*, 4268−4276. (c) Jin, N.; Bourassa, J. L.; Tizio, S. C.; Groves, J. T. Rapid, Reversible Oxygen Atom Transfer between an Oxomanganese-(V) Porphyrin and Bromide: A Haloperoxidase Mimic with Enzymatic Rates. *Angew. Chem., Int. Ed.* **2000**, *39*, 3849−3851. (d) Jin, N.; Groves, J. T. Unusual Kinetic Stability of a Ground-State Singlet Oxomanganese(V) Porphyrin. Evidence for a Spin State Crossing Effect. *J. Am. Chem. Soc.* **1999**, *121*, 2923−2924. (e) Groves, J. T.; Lee, J.; Marla, S. S. Detection and Characterization of an Oxomanganese(V) Porphyrin Complex by Rapid-Mixing Stopped-Flow Spectrophotometry. *J. Am. Chem. Soc.* **1997**, *119*, 6269−6273.

(5) (a) Fukuzumi, S.; Kishi, T.; Kotani, H.; Lee, Y.-M.; Nam, W. Highly Efficient Photocatalytic Oxygenation Reactions Using Water as an Oxygen Source. *Nat. Chem.* **2011**, *3*, 38−41. (b) Arunkumar, C.; Lee, Y.-M.; Lee, J. Y.; Fukuzumi, S.; Nam, W. Hydrogen-Atom Abstraction Reactions by Manganese(V)- and Manganese(IV)-Oxo Porphyrin Complexes in Aqueous Solution. *Chem. - Eur. J.* **2009**, *15*, 11482−11489. (c) Lee, J. Y.; Lee, Y.-M.; Kotani, H.; Nam, W.; Fukuzumi, S. High-Valent Manganese(V)-Oxo Porphyrin Complexes in Hydride Transfer Reactions. *Chem. Commun.* **2009**, 704−706. (d) Song, W. J.; Seo, M. S.; DeBeer George, S.; Ohta, T.; Song, R.; Kang, M.- J.; Tosha, T.; Kitagawa, T.; Solomon, E. I.; Nam, W. Synthesis, Characterization, and Reactivities of Manganese(V)-Oxo Porphyrin Complexes. *J. Am. Chem. Soc.* **2007**, *129*, 1268−1277. (e) Nam, W.; Kim, I.; Lim, M. H.; Choi, H. J.; Lee, J. S.; Jang, H. G. Isolation of an Oxomanganese(V) Porphyrin Intermediate in the Reaction of a Manganese(III) Porphyrin Complex and H_2O_2 in Aqueous Solution. *Chem. - Eur. J.* **2002**, *8*, 2067−2071.

(6) (a) Mann, S. I.; Nayak, A.; Gassner, G. T.; Therien, M. J.; DeGrado, W. F. *De Novo* Design, Solution Characterization, and Crystallographic Structure of an Abiological Mn−Porphyrin-Binding Protein Capable of Stabilizing a Mn(V) Species. *J. Am. Chem. Soc.* **2021**, *143*, 252−259. (b) Ma, Z.; Nakatani, N.; Hada, M. Insights into the Electronic Structure and Mechanism of Norcarane Hydroxylation by OxoMn(V) Porphyrin Complexes: A Density Functional Theory Study. *J. Comput. Chem.* **2021**, *42*, 1920−1928. (c) Ricciarelli, D.; Phung, Q. M.; Belpassi, L.; Harvey, J. N.; Belanzoni, P. Understanding the Reactivity of Mn-Oxo Porphyrins for Substrate Hydroxylation: Theoretical Predictions and Experimental Evidence Reconciled. *Inorg. Chem.* **2019**, *58*, 7345−7356. (d) Crestoni, M. E.; Fornarini, S.; Lanucara, F. Oxygen-Atom Transfer by a Naked Manganese(V)-Oxo-Porphyrin Complex Reveals Axial Ligand Effect. *Chem. - Eur. J.* **2009**, *15*, 7863−7866. (e) Zhang, R.; Horner, J. H.; Newcomb, M. Laser Flash Photolysis Generation and Kinetic Studies of Porphyrin-Manganese-Oxo Intermediates. Rate Constants for Oxidations Effected by Porphyrin-Mn^{V}-Oxo Species and Apparent Disproportionation Equilibrium Constants for Porphyrin−Mn^{IV}−Oxo Species. *J. Am. Chem. Soc.* **2005**, *127*, 6573−6582. (f) Zhang, R.; Newcomb, M. Laser Flash Photolysis Formation and Direct Kinetic Studies of Manganese(V)-Oxo Porphyrin Intermediates. *J. Am. Chem. Soc.* **2003**, *125*, 12418−12419.

(7) (a) Suga, M.; Akita, F.; Hirata, K.; Ueno, G.; Murakami, H.; Nakajima, Y.; Shimizu, T.; Yamashita, K.; Yamamoto, M.; Ago, H.; Shen, J.-R. Native Structure of Photosystem II at 1.95 Å Resolution Viewed by Femtosecond X-ray Pulses. *Nature* **2015**, *517*, 99−103. (b) Blakemore, J. D.; Crabtree, R. H.; Brudvig, G. W. Molecular Catalysts for Water Oxidation. *Chem. Rev.* **2015**, *115*, 12974−13005. (c) Zhang, B.; Sun, L. Artificial Photosynthesis: Opportunities and Challenges of Molecular Catalysts. *Chem. Soc. Rev.* **2019**, *48*, 2216−2264. (d) Zhang, X.-P.; Chandra, A.; Lee, Y.-M.; Cao, R.; Ray, K.; Nam, W. Transition Metal-Mediated O-O Bond Formation and Activation in Chemistry and Biology. *Chem. Soc. Rev.* **2021**, *50*, 4804−4811.

(8) (a) Gao, Y.; Åkermark, T.; Liu, J.; Sun, L.; Åkermark, B. Nucleophilic Attack of Hydroxide on a Mn^{V} Oxo Complex: A Model of the O−O Bond Formation in the Oxygen Evolving Complex of Photosystem II. *J. Am. Chem. Soc.* **2009**, *131*, 8726−8727. (b) Kim, S. H.; Park, H.; Seo, M. S.; Kubo, M.; Ogura, T.; Klajn, J.; Gryko, D. T.; Valentine, J. S.; Nam, W. Reversible O−O Bond Cleavage and Formation between Mn(IV)-Peroxo and Mn(V)-Oxo Corroles. *J. Am. Chem. Soc.* **2010**, *132*, 14030−14032. (c) Guo, M.; Lee, Y.-M.; Gupta, R.; Seo, M. S.; Ohta, T.; Wang, H.-H.; Liu, H.-Y.; Dhuri, S.-N.; Sarangi, R.; Fukuzumi, S.; Nam, W. Dioxygen Activation and O-O Bond Formation Reactions by Manganese Corroles. *J. Am. Chem. Soc.* **2017**, *139*, 15858−15867. (d) Li, X.; Zhang, X.-P.; Guo, M.; Lv, B.; Guo, K.; Jin, X.; Zhang, W.; Lee, Y.-M.; Fukuzumi, S.; Nam, W.; Cao, R. Identifying Intermediates in Electrocatalytic Water Oxidation with a Manganese Corrole Complex. *J. Am. Chem. Soc.* **2021**, *143*, 14613−14621.

(9) Abbreviations used: TDCPP, *meso*-tetrakis(2,6-dichlorophenyl)-porphinato dianion; HMPAB, 1,2-bis(2-hydroxy-2-methyl-propanamido)benzene; TPFC, 5,10,15-tris(pentafluorophenyl)-corrolato trianion; ^{S}PhIO, 1-(*tert*-butylsulfonyl)-2-iodosylbenzene; CAN, cerium(IV) ammonium nitrate; CSI-MS, cold spray ionization time-of-flight mass spectrum; rRaman, resonance Raman; EPR, electron paramagnetic resonance; XAS, X-ray absorption spectroscopy; EXAFS, extended X-ray absorption fine structure; XANES, X-ray absorption near edge structure; KIE, kinetic isotope effect; BDE, bond dissociation energy.

https://doi.org/10.1021/jacs.3c01818
J. Am. Chem. Soc. XXXX, XXX, XXX−XXX

(10) (a) Guo, M.; Seo, M. S.; Lee, Y.-M.; Fukuzumi, S.; Nam, W. Highly Reactive Manganese(IV)-Oxo Porphyrins Showing Temperature-Dependent Reversed Electronic Effect in C-H Bond Activation Reactions. *J. Am. Chem. Soc.* **2019**, *141*, 12187−12191. (b) Guo, M.; Zhang, J.; Zhang, L.; Lee, Y.-M.; Fukuzumi, S.; Nam, W. Enthalpy-Entropy Compensation Effect in Oxidation Reactions by Manganese-(IV)-Oxo Porphyrins and Nonheme Iron(IV)-Oxo Models. *J. Am. Chem. Soc.* **2021**, *143*, 18559−18570.

(11) It is noted that no observation of the Mn(III) porphyrin complex in the disproportionation reaction of **1** was due to the further oxidation of the Mn(III) porphyrin complex by ^{s}PhIO remaining in the reactions solution (Scheme 1A), as observed previously in the iron porphyrin and TAML systems: See refs 13a and 14a.

(12) (a) Nishikawa, K.; Honda, Y.; Fujii, H. Spectroscopic Evidence for Acid-Catalyzed Disproportionation Reaction of Oxoiron(IV) Porphyrin to Oxoiron(IV) Porphyrin π-Cation Radical and Iron(III) Porphyrin. *J. Am. Chem. Soc.* **2020**, *142*, 4980−4984. (b) Gupta, R.; Li, X.-X.; Lee, Y.; Seo, M. S.; Lee, Y.-M.; Yanagisawa, S.; Kubo, M.; Sarangi, R.; Cho, K.-B.; Fukuzumi, S.; Nam, W. Heme Compound II Models in Chemoselectivity and Disproportionation Reactions. *Chem. Sci.* **2022**, *13*, 5707−5717.

(13) (a) Pan, Z.; Newcomb, M. Acid-Catalyzed Disproportionation of Oxoiron(IV) Porphyrins to Give Oxoiron(IV) Porphyrin Radical Cations. *Inorg. Chem. Commun.* **2011**, *14*, 968−970. (b) Zhang, R.; Newcomb, M. Laser Flash Photolysis Generation of High-Valent Transition Metal−Oxo Species: Insights from Kinetic Studies in Real Time. *Acc. Chem. Res.* **2008**, *41*, 468−477. (c) Pan, Z.; Newcomb, M. Kinetics and Mechanism of Oxidation Reactions of Porphyrin−Iron(IV)−Oxo Intermediates. *Inorg. Chem.* **2007**, *46*, 6767−6774.

(14) (a) Lu, X.; Lee, Y.-M.; Seo, M. S.; Nam, W. Proton-Promoted Disproportionation of Iron(V)-Imido TAML to Iron(V)-Imido TAML Cation Radical and Iron(IV) TAML. *Chem. Commun.* **2020**, *56*, 11207−11210. (b) Wolak, M.; van Eldik, R. Mechanistic Studies on Peroxide Activation by a Water-Soluble Iron(III)-Porphyrin: Implications for O-O Bond Activation in Aqueous and Nonaqueous Solvents. *Chem. - Eur. J.* **2007**, *13*, 4873−4883.

(15) Such an interconversion between **1** and **2** upon adding acid and base has been demonstrated previously in high-valent iron-oxo (and iron-imido) species: See refs 12−14.

(16) (a) Bernadou, J.; Fabiano, A.-S.; Robert, A.; Meunier, B. Redox Tautomerism" in High-Valent Metal-oxo-aquo Complexes. Origin of the Oxygen Atom in Epoxidation Reactions Catalyzed by Water-Soluble Metalloporphyrins. *J. Am. Chem. Soc.* **1994**, *116*, 9375−9376. (b) Lee, K. A.; Nam, W. Determination of Reactive Intermediates in Iron Porphyrin Complex-Catalyzed Oxygenations of Hydrocarbons Using Isotopically Labeled Water: Mechanistic Insights. *J. Am. Chem. Soc.* **1997**, *119*, 1916−1922. (c) Seo, M. S.; In, J.-H.; Kim, S. O.; Oh, N. Y.; Hong, J.; Kim, J.; Que, L., Jr; Nam, W. Direct Evidence for Oxygen-Atom Exchange between Nonheme Oxoiron(IV) Complexes and Isotopically Labeled Water. *Angew. Chem., Int. Ed.* **2004**, *43*, 2417−2420.

(17) (a) Kitagawa, T.; Mizutani, Y. Resonance Raman Spectra of Highly Oxidized Metalloporphyrins and Heme Proteins. *Coord. Chem. Rev.* **1994**, *135*−*136*, 685−735. (b) Terner, J.; Palaniappan, V.; Gold, A.; Weiss, R.; Fitzgerald, M. M.; Sullivan, A. M.; Hosten, C. M. Resonance Raman Spectroscopy of Oxoiron(IV) Porphyrin π-Cation Radical and Oxoiron(IV) Hemes in Peroxidase Intermediates. *J. Inorg. Biochem.* **2006**, *100*, 480−501. (c) de Visser, S. P.; Rohde, J.-U.; Lee, Y.-M.; Cho, J.; Nam, W. Intrinsic Properties and Reactivities of Mononuclear Nonheme Iron-Oxygen Complexes Bearing the Tetramethylcyclam Ligand. *Coord. Chem. Rev.* **2013**, *257*, 381−393. (d) McDonald, A. R.; Que, L., Jr High-Valent Nonheme Iron-Oxo Complexes: Synthesis, Structure, and Spectroscopy. *Coord. Chem. Rev.* **2013**, *257*, 414−428.

(18) (a) Karmalkar, D. G.; Sankaralingam, M.; Seo, M. S.; Ezhov, R.; Lee, Y.-M.; Pushkar, Y. N.; Kim, W.-S.; Fukuzumi, S.; Nam, W. A High-Valent Manganese(IV)-Oxo-Cerium(IV) Complex and Its Enhanced Oxidizing Reactivity. *Angew. Chem., Int. Ed.* **2019**, *58*, 16124−16129. (b) Draksharapu, A.; Rasheed, W.; Klein, J. E. M. N.; Que, L., Jr Facile and Reversible Formation of Iron(III)-Oxo-Cerium(IV) Adducts from Nonheme Oxoiron(IV) Complexes and Cerium(III). *Angew. Chem., Int. Ed.* **2017**, *56*, 9091−9095. (c) Codolà, Z.; Gómez, L.; Kleespies, S. T.; Que, L., Jr; Costas, M.; Lloret-Fillol, J. Evidence for an Oxygen Evolving Iron-Oxo-Cerium Intermediate in Iron-Catalysed Water Oxidation. *Nat. Commun.* **2015**, *6*, No. 5865.

(19) (a) Lee, Y.; Tripodi, G. L.; Jeong, D.; Lee, S.; Roithova, J.; Cho, J. Aliphatic and Aromatic C-H Bond Oxidation by High-Valent Manganese(IV)-Hydroxo Species. *J. Am. Chem. Soc.* **2022**, *144*, 20752−20762. (b) Park, Y.; Kim, S.; Kim, K.; Shin, B.; Jang, Y.; Cho, K.-B.; Cho, J. Structure and Reactivity of Nonporphyrinic Terminal Manganese(IV)-Hydroxide Complexes in the Oxidative Electrophilic Reaction. *Inorg. Chem.* **2022**, *61*, 4292−4301. (c) Karmalkar, D. G.; Seo, M. S.; Lee, Y.-M.; Kim, Y.; Lee, E.; Sarangi, R.; Fukuzumi, S.; Nam, W. Deeper Understanding of Mononuclear Manganese(IV)-Oxo Binding Brønsted and Lewis Acids and the Manganese(IV)-Hydroxide Complex. *Inorg. Chem.* **2021**, *60*, 16996−17007. (d) Zaragoza, J. P. T.; Siegler, M. A.; Goldberg, D. P. A Reactive Manganese(IV)-Hydroxide Complex: A Missing Intermediate in Hydrogen Atom Transfer by High-Valent Metal-Oxo Porphyrinoid Compounds. *J. Am. Chem. Soc.* **2018**, *140*, 4380−4390. (e) Garcia-Bosch, I.; Company, A.; Cady, C. W.; Styring, S.; Browne, W. R.; Ribas, X.; Costas, M. Evidence for a Precursor Complex in C-H Hydrogen Atom Transfer Reactions Mediated by a Manganese(IV) Oxo Complex. *Angew. Chem., Int. Ed.* **2011**, *50*, 5648−5653. (f) Yin, G.; McCormick, J. M.; Buchalova, M.; Danby, A. M.; Rodgers, K.; Day, V. W.; Smith, K.; Perkins, C. M.; Kitko, D.; Carter, J. D.; Scheper, W. M.; Busch, D. H. Synthesis, Characterization, and Solution Properties of a Novel Cross-Bridged Cyclam Manganese(IV) Complex Having Two Terminal Hydroxo Ligands. *Inorg. Chem.* **2006**, *45*, 8052−8061.

(20) (a) Song, W. J.; Seo, M. S.; George, S. D.; Ohta, T.; Song, R.; Kang, M.-J.; Tosha, T.; Kitagawa, T.; Soloman, E. I.; Nam, W. Synthesis, Characterization, and Reactivities of Manganese(V)-Oxo Porphyrin Complexes. *J. Am. Chem. Soc.* **2007**, *129*, 1268−1277. (b) Westre, T. E.; Kennepohl, P.; DeWitt, J. G.; Hedman, B.; Hodgson, K. O.; Solomon, E. I. A Multiplet Analysis of Fe K-Edge 1s-3d Pre-Edge Features of Iron Complexes. *J. Am. Chem. Soc.* **1997**, *119*, 6297−6314. (c) Guo, M.; Lee, Y.-M.; Gupta, R.; Seo, M. S.; Ohta, T.; Wang, H.-H.; Liu, H.-Y.; Dhuri, S. N.; Sarangi, R.; Fukuzumi, S.; Nam, W. Dioxygen Activation and O-O Bond Formation Reactions by Manganese Corroles. *J. Am. Chem. Soc.* **2017**, *139*, 15858−15867.

(21) It has been demonstrated in metal-oxo complexes, including Mn(IV)-oxo, that binding of Lewis and Brønsted acids at the metal-oxo moiety elongates the metal-oxo bond length, although the change of the metal-oxo stretch by binding of Lewis and Brønsted acids has never been reported previously: (a) Mayfield, J. R.; Grotemeyer, E. N.; Jackson, T. A. Concerted Proton-Electron Transfer Reactions of Manganese-Hydroxo and Manganese-Oxo Complexes. *Chem. Commun.* **2020**, *56*, 9238−9255. (b) Devi, T.; Lee, Y.-M.; Nam, W.; Fukuzumi, S. Metal Ion-Coupled Electron-Transfer Reactions of Metal-Oxygen Complexes. *Coord. Chem. Rev.* **2020**, *410*, 213219. (c) Liu, Y.; Lau, T.-C. Activation of Metal Oxo and Nitrido Complexes by Lewis Acids. *J. Am. Chem. Soc.* **2019**, *141*, 3755−3766. (d) Cook, S. A.; Borovik, A. S. Molecular Designs for Controlling the Local Environments around Metal Ions. *Acc. Chem. Res.* **2015**, *48*, 2407−2414. (e) Chen, J.; Yoon, H.; Lee, Y.-M.; Seo, M.-S.; Sarangi, R.; Fukuzumi, S.; Nam, W. Tuning the Reactivity of Mononuclear Nonheme Manganese(IV)-Oxo Complexes by Triflic Acid. *Chem. Sci.* **2015**, *6*, 3624−3632. (f) Chen, J.; Lee, Y.-M.; Davis, K. M.; Wu, X.; Seo, M. S.; Cho, K.-B.; Yoon, H.; Park, Y. J.; Fukuzumi, S.; Pushkar, Y. N.; Nam, W. A Mononuclear Non-Heme Manganese(IV)-Oxo Complex Binding Redox-Inactive Metal Ions. *J. Am. Chem. Soc.* **2013**, *135*, 6388−6391.

(22) The reactivity differences of Mn(IV)-oxo and Mn(IV)-hydroxo complexes bearing a common supporting ligand have been compared in a nonheme system: (a) Yin, G. Understanding the Oxidation Relationships of the Metal Oxo, Hydroxo, and Hydroperoxide Intermediates with Manganese(IV) Complexes Having Bridged

https://doi.org/10.1021/jacs.3c01818
J. Am. Chem. Soc. XXXX, XXX, XXX−XXX

Cyclams: Correlation of the Physicochemical Properties with Reactivity. *Acc. Chem. Res.* **2013**, *46*, 483−492. (b) Shi, S.; Wang, Y.; Xu, A.; Wang, H.; Zhu, D.; Roy, S. B.; Jackson, T. A.; Busch, D. H.; Yin, G. Distinct Reactivity Differences of Metal Oxo and Its Corresponding Hydroxo Moieties in Oxidations: Implications from a Manganese(IV) Complex Having Dihydroxide Ligand. *Angew. Chem., Int. Ed.* **2011**, *50*, 7321−7324. (c) Xu, A.; Xiong, H.; Yin, G. Distinct Oxygenation Difference between Manganese(IV) Hydroxo and Oxo Moieties: Electron Transfer versus Concerted Oxygen Transfer. *Chem. - Eur. J.* **2009**, *15*, 11478−11481. (d) Yin, G.; Danby, A. M.; Kitko, D.; Carter, J. D.; Scheper, W. M.; Busch, D. H. Oxidative Reactivity Difference among the Metal Oxo and Metal Hydroxo Moieties: pH Dependent Hydrogen Abstraction by a Manganese(IV) Complex Having Two Hydroxide Ligands. *J. Am. Chem. Soc.* **2008**, *130*, 16245−16253.

(23) Fukuzumi, S.; Lee, Y.-M.; Nam, W. Deuterium Kinetic Isotope Effects as Redox Mechanistic Criterions. *Bull. Korean Chem. Soc.* **2021**, *42*, 1558−1568.

(24) Luo, Y. R. *Handbook of Bond Dissociation Energies in Organic Compounds*; CRC Press: Boca Raton, 2003.

(25) (a) Huang, X.; Groves, J. T. Beyond Ferryl-Mediated Hydroxylation: 40 Years of the Rebound Mechanism and C−H Activation. *J. Biol. Inorg. Chem.* **2017**, *22*, 185−207. (b) Cho, K.-B.; Hirao, H.; Shaik, S.; Nam, W. To Rebound or Dissociate? This is the Mechanistic Question in C−H Hydroxylation by Heme and Nonheme Metal−Oxo Complexes. *Chem. Soc. Rev.* **2016**, *45*, 1197−1210.

(26) (a) Duan, L.; Wang, L.; Li, F.; Sun, L. Highly Efficient Bioinspired Molecular Ru Water Oxidation Catalysts with Negatively Charged Backbone Ligands. *Acc. Chem. Res.* **2015**, *48*, 2084−2096. (b) Garrido-Barros, P.; Gimbert-Suriñach, C.; Matheu, R.; Sala, X.; Llobet, A. How to Make an Efficient and Robust Molecular Catalyst for Water Oxidation. *Chem. Soc. Rev.* **2017**, *46*, 6088−6098. (c) Casadevall, C.; Martin-Diaconescu, V.; Browne, W. R.; Fernández, S.; Franco, F.; Cabello, N.; Benet-Buchholz, J.; Lassalle-Kaiser, B.; Lloret-Fillol, J. Isolation of a Ru(IV) Side-On Peroxo Intermediate in the Water Oxidation Reaction. *Nat. Chem.* **2021**, *13*, 800−804.

https://doi.org/10.1021/jacs.3c01818
J. Am. Chem. Soc. XXXX, XXX, XXX−XXX